

# The *Drosophila ovarian tumor* Gene Is Required for the Organization of Actin Filaments during Multiple Stages in Oogenesis

Christopher Rodesch, Janette Pettus, and Rod N. Nagoshi

Department of Biological Sciences, University of Iowa, Iowa City, Iowa 52242-1234

**The *ovarian tumor* gene is required during both early and late stages of oogenesis. Mutations produce a range of phenotypes, including agametic ovarioles, tumorous egg chambers, and late stage oogenic arrest. We demonstrate that each of these phenotypes is associated with specific aberrations in actin distribution. In the earliest case, *ovarian tumor* mutations cause actin filaments to accumulate ectopically in the fusome. This correlates with abnormal fusome morphology and arrested germ cell development in the germaria. Similarly, *ovarian tumor* function is required for the localization of actin that is essential for the maturation of ring canals. This defect gives rise to tumorous egg chambers in which germ cell numbers and morphology are profoundly aberrant. We also confirm that *ovarian tumor* is required for the formation of the nurse cell cytoplasmic actin array that is essential for the nonspecific transport of cytoplasmic contents to the oocyte during late oogenesis. Our data suggest that at this stage *ovarian tumor* controls the site where actin filaments initiate. Taken together, these studies suggest that the diverse *ovarian tumor* mutant phenotypes derive from the mislocalization of actin filaments, indicating a role for this gene in organizing the female germline cytoskeleton, and that the misregulation of actin can have profound effects on germ cell division and differentiation.** © 1997 Academic Press

## INTRODUCTION

The adult *Drosophila* ovary consists of two lobes each containing approximately 15 elongated tubes called ovarioles (reviewed in King, 1970; Mahowald and Kambyzellis, 1980; Spradling, 1993). The formation of the egg chamber occurs in the germarium, located at the distal tip of the ovariole, which is subdivided into three morphologically distinct regions. In region I, germline stem cells produce cystoblasts that are programmed to undergo four sets of mitotic divisions to produce 16 cystocytes, each connected by intercellular bridges or ring canals. In region II, somatic mesenchymal cells, the presumptive follicle layer, migrate to and envelop the newly formed 16-cell cyst until, by region III, a single follicle cell monolayer surrounds and separates the cyst from the rest of the germaria. This is defined as a stage 1 egg chamber, the first of 14 vitellogenic stages (King, 1970).

A prominent feature of germ cell differentiation is the formation of the cytoplasmic bridges connecting the cystocytes (reviewed in Robinson *et al.*, 1994). In germarial region I, stem cells and cystoblasts contain a spectrin-rich body known as the spectroosome (Lin *et al.*, 1994). As the cystoblast divides, the spectroosome gives rise to an elongated

structure called the fusome that extends through the ring canals to form branched connections between daughter cystocytes (Spradling, 1993, Lin *et al.*, 1994). Some components of the fusome have been identified, including the product of the *hu-li tai shao* (*hts*) gene,  $\alpha$ -spectrin, *bag-of-marbles* (*bam*), and a protein with a phosphotyrosine epitope (Spradling, 1993; Lin *et al.*, 1994; Robinson *et al.*, 1994; McKearin and Ohlstein, 1995). The fusome is not required for ring canal formation, but may play a role in controlling the orientation of mitotic spindles, regulating cystocyte proliferation, and determining the oocyte (Lin *et al.*, 1994; Lin and Spradling, 1995).

The fusome regresses and disappears by the middle of germarial region II, clearing a passageway for cytoplasmic exchange between cystocytes (Lin *et al.*, 1994; Robinson *et al.*, 1994). This occurs coincident with the deposition of actin filaments and Hts protein to the inner surface of the ring canals, forming a thick layer called the inner rim. Subsequent maturation of the ring canal requires the later association of the Kelch protein, which is believed to be involved in actin bundling (Robinson *et al.*, 1994).

The actin cytoskeleton continues to play a major role in the maturation of the egg chamber during later oogenic stages. A dramatic doubling of oocyte size occurs from stage

10 to stage 11 due to the rapid, nonspecific transport of nurse cell cytoplasmic contents. This process, called nurse cell dumping, occurs through a myosin-dependent contraction of nurse cells which force material through the ring canals into the oocyte (Edwards and Kiehart, 1996). A dense array of cytoplasmic actin filaments form in the nurse cells during stage 10 (Warn *et al.*, 1985), anchoring the nuclei such that they do not float to and physically impede flow through the ring canals (Cooley *et al.*, 1992; Mahajan-Miklos and Cooley, 1994).

Mutations in the *ovarian tumor (otu)* gene disrupt germarial and vitellogenic stages of oogenesis, producing a complex array of oogenic defects that have been subdivided into three classes (King *et al.*, 1986; King and Storto, 1988). The agametic phenotype is characterized by the absence of egg chambers in a given ovariole. The tumorous class refers to a type of egg chamber in which an apparently normal follicle layer surrounds hundreds of mostly undifferentiated germ cells (King and Riley, 1982; Bishop and King, 1984). Both agametic ovarioles and tumorous egg chambers are produced in *otu* null mutants (Geyer *et al.*, 1993), while tumors predominate in some hypomorphic allele combinations (King and Riley, 1982; King *et al.*, 1986). In the least severe phenotypic class ("differentiated" chambers), egg chambers mature to approximately stage 10, as defined by the size of the oocyte relative to the egg chamber (King and Riley, 1982). This arrest is not complete, however, as in many cases the morphologies of individual germ and follicle cells in these chambers are more consistent with stage 12 or later development (King *et al.*, 1986).

How *otu* functions in oogenesis is not known. Similarity in the amino acid sequence of *otu* has been reported to short regions of *bam*, a gene of unknown function localized in fusomes and required for male and female gametogenesis (McKearin and Spradling, 1990; McKearin and Ohlstein, 1995), and to parts of a mouse microtubule-associated protein (Tirronen *et al.*, 1995). However, in both cases the sequence similarity is weak and not to conserved domains of known function. The cytological localization of *otu* product has also been inconclusive as it has a broad cytoplasmic distribution and no association of *Otu* protein with specific organelles or proteins has yet been demonstrated (Sass *et al.*, 1995).

One proposed mechanism for *otu* function is that it controls germline sex determination (Steinmann-Zwicky, 1992; Oliver *et al.*, 1993; Pauli *et al.*, 1993; Wei *et al.*, 1994). This is based on morphological similarities of tumorous germ cells to primary spermatocytes and the misregulation of certain sex-specific genes in *otu* mutant tumors. Alternatively, electron microscopic reconstructions of *otu* mutant tumorous cells detected abnormal patterns of cytoplasmic connections and morphologically aberrant fusomes, perhaps indicating a role for *otu* in stabilizing fusome structure (King, 1979; King *et al.*, 1986). During later oogenesis, *otu* is required for nurse cell dumping and appears to be needed for the formation of the actin cytoplasmic array in stage 10 nurse cells (Storto and King, 1988). More recently, *otu*

mutants were shown to disrupt the cellular localization of specific maternal RNAs in later oogenic stages, implicating an effect on microtubule organization or function (Tirronen *et al.*, 1995). While all of these proposals are intriguing, they fail to provide a comprehensive explanation for the variety of *otu* effects on germ cell number and differentiation in early and late stages of oogenesis.

In this paper, we examine the effects of *otu* mutations at different times in oogenesis, including providing the first detailed analysis of the *otu* null phenotype. We demonstrate that mutations in *otu* can block the differentiation of cystocytes at two different germarial stages, each resulting in a similar ovarian tumor phenotype. In both cases, the mutant cystocytes have fusome and ring canal abnormalities coincident with the aberrant localization or formation of actin filaments. We also confirm that *otu* is required to form the cytoplasmic actin array in stage 10 nurse cells and further show evidence for mislocalization of actin during this period. These data provide the first molecular linkage between the early and late *otu* oogenic phenotypes.

## MATERIAL AND METHODS

**Genotypes and allelic information.** The *otu*<sup>P<sup>Δ</sup>1</sup> allele is a homozygous viable deletion of the entire *otu* coding region (Geyer *et al.*, 1993; Sass *et al.*, 1993). *otu*<sup>P<sup>Δ</sup>3</sup> and *otu*<sup>P<sup>Δ</sup>5</sup> are deletions in the promoter and untranslated portions of the *otu* gene (Geyer *et al.*, 1993; Sass *et al.*, 1993). *otu*<sup>5</sup>, *otu*<sup>7</sup>, *otu*<sup>13</sup>, and *otu*<sup>14</sup> are point mutations (King and Riley, 1982; Lindsley and Zimm, 1992; Steinhauer and Kalfayan, 1992).

**Ovary dissection and fixation.** Ovaries from adults aged 4–6 days were dissected in PBS (130 mM NaCl, 7 mM Na<sub>2</sub>HPO<sub>4</sub>–2H<sub>2</sub>O, 3 mM NaH<sub>2</sub>PO<sub>4</sub>–2H<sub>2</sub>O) and ovarioles were teased apart with tungsten needles. Ovaries were placed in a dissection slide and fixed with a 1:1 solution of fix:heptane (fix: 4% paraformaldehyde in PBS) for 20 min with agitation. The fix:heptane solution was removed by aspiration and the preparation washed three times for 10 min with PBT (0.1% Triton X-100, 0.05% Tween 80 in PBS). The fixed preparation was now ready for labeling.

**Phalloidin staining.** Fixed preparations were incubated with 1–2 units of either Texas red- or rhodamine-conjugated phalloidin for 30 min (Molecular Probes). Three 10-min washes in PBT were used to remove excess phalloidin. Ovaries were then mounted in 70% glycerol with 1 mg/ml DABCO (Sigma) antifade reagent.

**Antibody protocol.** Fixed ovaries were permeabilized in PBTBS (PBT + 1 mg/ml crystalline BSA, Sigma) for 2–4 hr at room temperature. Primary antibodies were diluted in PBTBS and incubated with ovaries at 4°C overnight. Primaries used included anti-phosphotyrosine (No. PY20, Signal Analytics) at 1:200 dilution, anti- $\alpha$ -spectrin (gift of D. Branton) at 1:200 dilution, and anti-Hts (gift of D. Robinson and L. Cooley) at 1:200 dilution. Primary antibodies were washed off with three 10-min washes in PBT. Preparations were incubated with secondary antibodies (diluted 1:200 in PBTBS) for either 2 hr at room temperature or overnight at 4°C. Secondary antibodies used included biotinylated anti-mouse IgG (Sigma), biotinylated anti-rabbit (Sigma), and rhodamine-conjugated anti-mouse IgG (Sigma). Preparations were fluorescently labeled using fluorescent streptavidin reagents diluted 1:200 in PBT blocking solution and incubated with the ovaries for 30 min. After washing

with PBT, ovaries were mounted in 70% glycerol with 1 mg/ml DABCO (Sigma).

**Confocal microscopy.** Images were obtained on a Nikon Optiphot using a Bio-Rad MRC 1024 confocal laser apparatus. Sections were manipulated using Bio-Rad LaserSharp image analysis software.

**Transmission electron microscopy.** Ovaries were dissected from 6-day-old females in  $1\times$  PBS, pH 7.4, immediately prior to fixation. Intact ovary lobes were fixed for 1 hr in a modified Trumps universal fixative (Trumps: 1% glutaraldehyde, 4% formaldehyde, 1% tannic acid in 0.1 M Na cacodylate buffer, pH 7.2–7.4), passed through a secondary 1-hr fixation step in 1%  $\text{OsO}_4$  in 0.1 M Na cacodylate buffer, pH 7.2, en bloc stained for 20 min with 2% uranyl acetate, and dehydrated in acetone. The fixed ovaries were infiltrated with EMBED 812 resin and polymerized for 24 hr in a 60°C oven. Semithin sections of  $800\text{ nm}^{-1}\ \mu\text{m}$  were cut, stained with Richardson's stain, and viewed and photographed on an Olympus Vanox AHB3 light microscope. Thin sections of 90–150 nm were poststained with uranyl acetate and Reynolds lead and examined on a Philips EM300 electron microscope (Reynolds, 1963). Longitudinal sections were cut at 20- to 30- $\mu\text{m}$  intervals from two or more ovary lobes for each genotype examined. Twenty to 30 thin sections were cut and mounted on grids for each interval.

## RESULTS

The most severe alleles of *otu* frequently produce adult ovaries devoid of egg chambers. It had generally been assumed that these agametic ovaries lack germ cells (King and Riley, 1982; Pauli *et al.*, 1993). However, we demonstrated that *otu* null germ cells survive to the adult stage (Rodesch *et al.*, 1995). This provided an opportunity to determine (1) the earliest oogenic stage affected by the absence of *otu*, (2) the latest stage of differentiation attained by the majority of these mutant cells, and (3) specific cellular structures and processes affected.

### *otu* Null Alleles Arrest Oogenesis in Germarial Regions I and II

We compared the morphology of wild-type germaria to those of flies homozygous for the *otu*<sup>PΔ1</sup> allele, a deletion of the *otu* coding region. Mutant flies are female-sterile and produce either agametic ovarioles or tumorous egg chambers. The frequency of either phenotype can vary between ovaries and within ovarioles of a single ovary, suggesting a stochastic element to the null phenotype. In wild-type ovaries, germarial region I contains mitotically active stem cells, cystoblasts, and a few cystocyte clusters in the process of reaching the 16-cell stage (Fig. 1A; King, 1970). In region II, the 16-cell cysts become separated by migrating follicle cells, eventually forming individual egg chambers by region III. We found that the *otu*<sup>PΔ1</sup> mutation causes enlargement of germarial region I, resulting from an increased number of germ cells arrested at stages prior to when they would normally interact with follicle cells (Fig. 1B).

To better determine the stage of arrest of the mutant germ cells we examined the intracellular distributions of spectrin

and actin. Spectrin is found in the spectrosomes of oogonial stem cells and cystoblasts and in the fusomes of the dividing cystocytes, whereas actin filaments are present cortically in region I germ cells but had not previously been detected in spectrosomes or fusomes (Warn *et al.*, 1985; Lin *et al.*, 1994). By using Texas red-conjugated phalloidin (a more sensitive probe for actin filaments than those used in previous studies), we consistently detected actin filaments in the spectrosomes of wild-type oogonial stem cells and cystoblasts (Fig. 1C), colocalizing with spectrin antibodies (data not shown). Similar germ cells lacking ring canals and with prominent spectrosomes were found in *otu*<sup>PΔ1</sup> mutant tumorous egg chambers (Fig. 1D). This confirms that the *otu* null allele arrests oogenesis prior to the first cystocyte division, with a consequent accumulation of these cells in germaria and tumorous chambers.

A second type of mutant germ cell was commonly found that had undergone at least one mitotic division, as detected by a phosphotyrosine-specific antibody that detects one of the earliest ring canal components (Fig. 1E; Robinson *et al.*, 1994). As with the spectrosome-containing cell type, those with ring canals were found in substantial, but variable, proportions in both agametic ovarioles and tumorous egg chambers. We examined these mutant cystocytes by electron microscopy and found that they generally had undergone a single cystocyte division, as cells with two or more ring canals were only rarely observed.

The morphology of these mutant ring canals was consistent with an arrest early in oogenesis. In a cross-section of a wild-type region I ring canal (a diagram of the type of section examined is illustrated in Fig. 2G), the ring canal wall forms a thickened L-shaped rim extending orthogonally from the plasma membrane (Fig. 2A, arrows). In every case examined at this stage ( $n = 9$ ) these rims were positioned in opposite orientation. The fusome, a vesiculated, proteinaceous structure, runs through the ring canals (Fig. 2A, fu; Mahowald, 1971; Mahowald and Kambyzellis, 1980; Lin *et al.*, 1994). Several morphological changes occur in the ring canals in region II that distinguish them from those in region I. The fusome disappears, allowing intercellular exchange of cytoplasm and organelles, coincident with the formation of an electron-dense layer (the inner rim) on the inner surface of the ring canal wall (Fig. 2B; Meyer *et al.*, 1961; Koch and King, 1969). A subset of region II ring canals also now have their rims oriented in the same direction (Fig. 2B). This change in rim direction is part of ring maturation, since the opposite orientation was no longer observed in postregion II stages ( $n > 20$ ).

Electron microscopy sections of *otu*<sup>PΔ1</sup> mutant ring canals ( $n > 20$ ) showed that they lacked inner rims, had outer rims in opposite orientation, and were associated with fusomes (Fig. 2C). The same phenotypes were found in mutant cystocytes from both agametic ovarioles and tumorous egg chambers. Taken together, these data indicate that in the absence of *otu* activity, the female germline will generally undergo no more than one cystocyte division and fail to differentiate beyond stages normally associated with germarial region I.

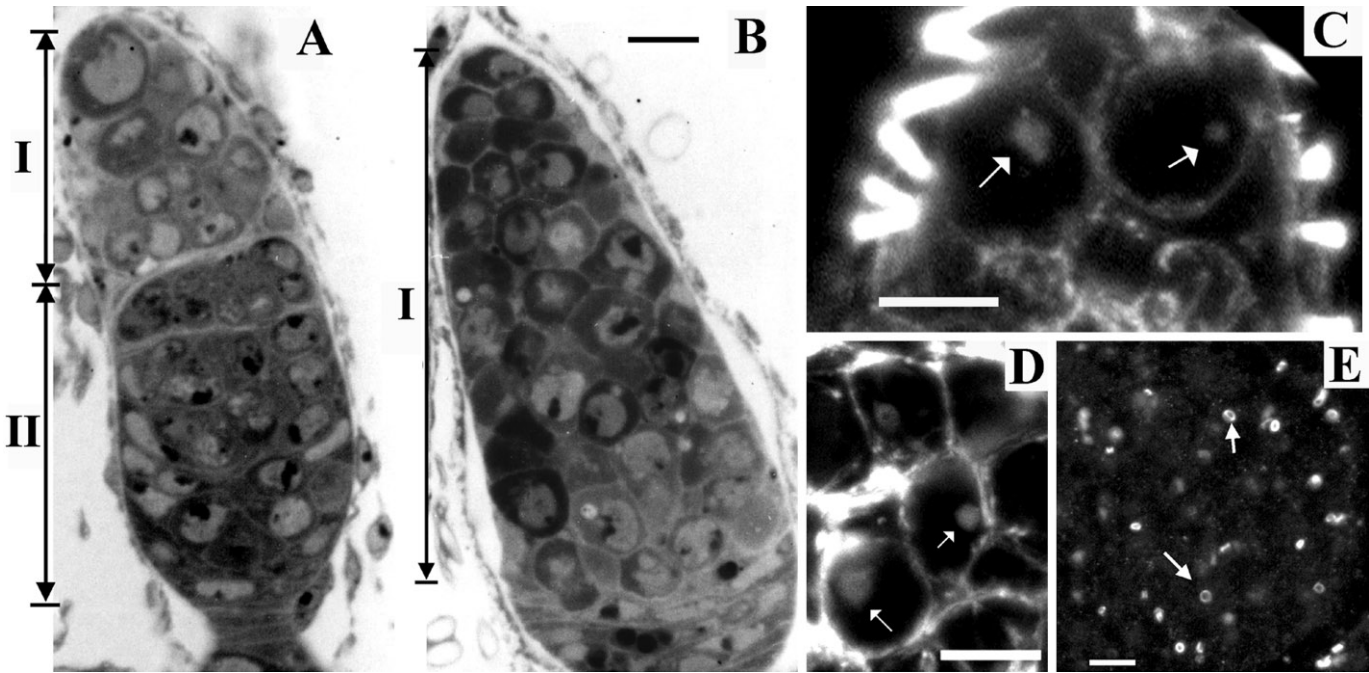


**FIG. 1.** Comparisons of *otu*<sup>PΔ1</sup> and wild-type early germ cells. (A) Thick section of wild-type germaria stained with Richardson's stain. Germarial regions I and II are indicated. Region II is defined by migrating somatic cells that separate the germline cysts. (B) Germaria from *otu*<sup>PΔ1</sup> mutant ovary. Note expansion of region I. (A) and (B) are at same magnification; size bar equals 10 μm. (C) Confocal image of wild-type germ cells from germaria labeled with Texas red-phalloidin. Arrows indicate spectrosomes containing actin. (D) Confocal image of *otu*<sup>PΔ1</sup> cells from tumorous chamber labeled with Texas red-phalloidin. Arrows indicate spectrosomes. (E) Lower magnification confocal image of *otu*<sup>PΔ1</sup> cells from a tumorous chamber labeled with anti-phosphotyrosine. Arrows indicate ring canals. For C-E, size bars equal 10 μm.

The formation of an egg chamber requires the migration of the follicle cell layer to encapsulate a germ cell cyst. This normally occurs shortly after the 16-cystocyte stage, suggesting that cystocytes must reach a certain maturity before they can interact with somatic follicle cells. Although *otu*<sup>PΔ1</sup> appears to arrest oogenesis prior to this stage, egg chambers (albeit tumorous) could still form in this mutant. We compared the germ cells in agametic ovarioles to those in tumorous chambers and could find no obvious differences in either cell morphology or the number of ring canals. It therefore appears that immature germ cells can interact with follicle cells, although chamber formation is variable.

### **Hypomorphic Tumorous *otu* Alleles Block a Later Stage of Oogenesis**

Severe hypomorphic alleles of *otu* form primarily tumorous egg chambers that superficially resemble the tumors produced by the *otu*<sup>PΔ1</sup> null mutation. However, genetic studies indicate differences between these tumorous cells in their interactions with the *Sexlethal* (*Sxl*) gene, suggesting a different stage of arrest (Pauli *et al.*, 1993; Bae *et al.*, 1994; see Discussion). Two such hypomorphic alleles are *otu*<sup>13</sup>

and *otu*<sup>PΔ3</sup> (King and Riley, 1982; Geyer *et al.*, 1993). The *otu*<sup>13</sup> allele is a point mutation in the 5' splice acceptor site of the alternatively spliced exon (Steinhauer *et al.*, 1989), while the *otu*<sup>PΔ3</sup> allele is a small deletion in the *otu* promoter region (Geyer *et al.*, 1993; Sass *et al.*, 1993). We examined the morphology of the tumorous cells produced by these alleles and compared them to each other and to *otu*<sup>PΔ1</sup>.

For both *otu*<sup>13</sup> and *otu*<sup>PΔ3</sup> alleles, between 70 and 90% of the egg chambers are completely tumorous, with most of the remainder containing a mixture of tumorous and a few nurse-like cells (King *et al.*, 1986; Geyer *et al.*, 1993). Many of the ring canals found in tumorous cells are morphologically identical to those of wild-type region II cystocytes. Figure 2D is a glancing section through the rim wall of an *otu*<sup>13</sup> ring canal that highlights the inner rim structure (diagrammed in Fig. 2H). These ring canals are devoid of fusome material and have inner rims that are indistinguishable from wild type. Similar ring canals were found in *otu*<sup>PΔ3</sup> preparations (data not shown). These observations indicate that both *otu*<sup>PΔ3</sup> and *otu*<sup>13</sup> mutant germ cells can undergo further differentiation than *otu*<sup>PΔ1</sup> mutants, appearing to reach stages associated with region II when germ cells normally interact with the migrating follicle cell layer. This is consistent with the higher frequency of egg chamber forma-

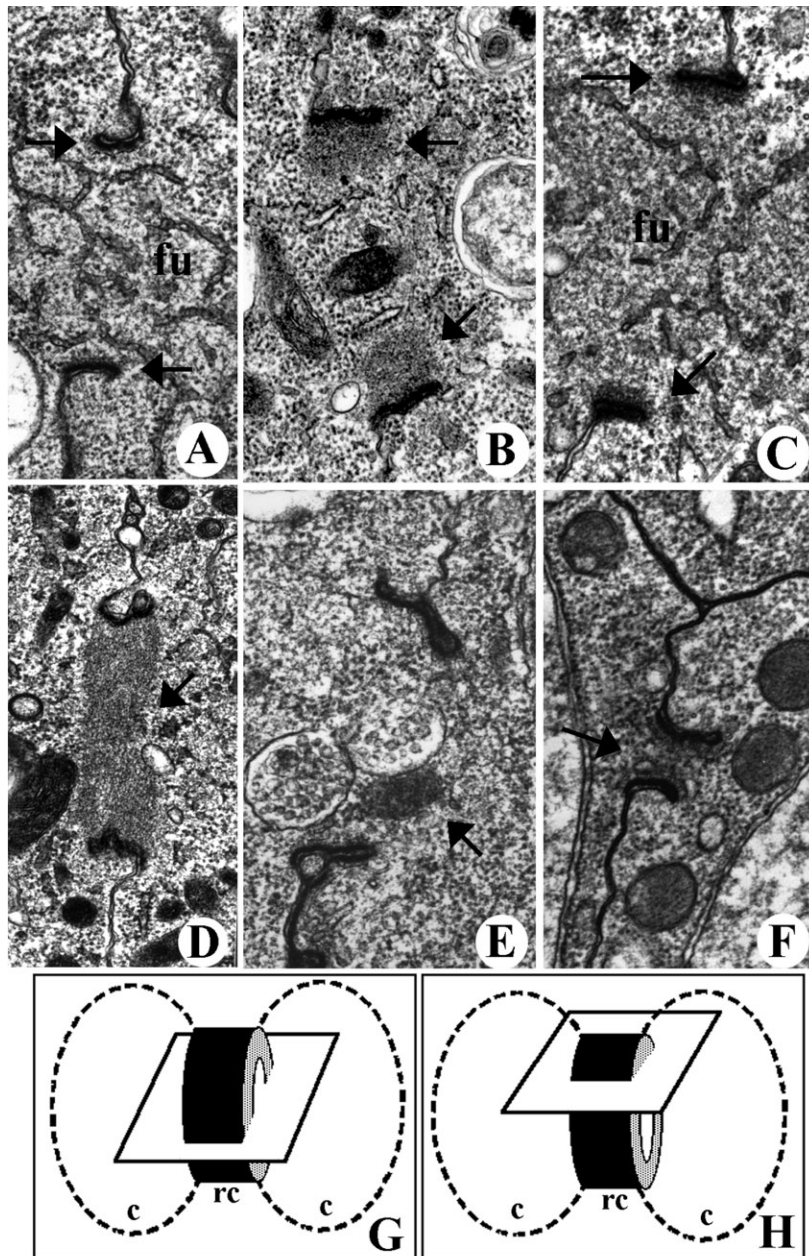


**FIG. 2.** Electron micrographs of ring canals and fusomes. (A) Cross-section of a ring canal from wild-type germarial region I. Arrows indicate electron opaque outer rim wall. Note that the walls extend from the plasma membrane in L-shaped structures pointed in opposite directions. The fusome (fu) is a proteinaceous region that is devoid of ribosomes and mitochondria and contains many prominent vesicles. (B) A ring canal from wild-type germarial region II. Arrows indicate the electron dense inner rim on the inner surface of the ring canal wall. Absence of fusome is noted by organelles passing through the ring canal. Note that the two outer rim walls extend from the plasma membrane in the same direction. (C) A ring canal from *otu*<sup>PA1</sup> tumorous cell. Arrows indicate outer rim wall. (D) A ring canal from *otu*<sup>13</sup> tumorous cell. This is a glancing section through the rim wall that does not include the central canal. (E) A ring canal from *otu*<sup>13</sup> tumorous cell. Arrow points to organelle moving through the ring canal. Note lack of fusome and inner rims. (F) A miniring canal from *otu*<sup>PA3</sup> cells in a tumorous egg chamber. Arrow points to canal that lacks fusome and inner rim. (G) Diagram of cross-section of ring canal depicted in A-C and E and F. (H) Diagram of cross-section of ring canal depicted for D. For A-F, original magnification is at 40,000 $\times$ .

tion in *otu*<sup>PΔ3</sup> and *otu*<sup>13</sup> compared to *otu*<sup>PΔ1</sup> mutants (King *et al.*, 1986; Geyer *et al.*, 1993). However, despite their more mature state most *otu*<sup>PΔ3</sup> or *otu*<sup>13</sup> germ cells still displayed the tumorous phenotype and still had no more than one ring canal.

Two other aberrant types of ring canals were also frequently observed in *otu*<sup>PΔ3</sup> and *otu*<sup>13</sup> mutants. In one case, the ring canals lacked both fusomes and an inner ring (Fig. 2E, compare to wild type in Fig. 2B). We have not seen ring canals of this type in wild-type preparations, where the loss of the fusome occurs concomitantly with the deposition of the inner rim. In addition, a number of *otu*<sup>PΔ3</sup> ring canals were only a fraction of the size of those found in wild-type or *otu*<sup>PΔ1</sup> cystocytes (Fig. 2F). These "minirings" lacked fusomes and inner rims. Similar minirings were also occasionally found in *otu*<sup>13</sup> chambers, although less frequently than with *otu*<sup>PΔ3</sup>.

### The *otu* Null Mutation Disrupts Actin Organization in Developing Cystocytes

To further investigate the differentiation of *otu* mutant germ cells, we double-labeled ovaries with Texas red-conjugated phalloidin, under conditions that allowed detection of actin in spectrosomes (Fig. 1C), and anti-spectrin antibodies. Figure 3A depicts a wild-type branched fusome labeled with anti-spectrin, while in the same preparation the partial outlines of four cells can be seen in the phalloidin channel due to labeling of cortical actin (Fig. 3B). The overlay indicates that this fusome connects four cystocytes (Fig. 3C). We could detect no phalloidin staining in the fusome at any stage (Fig. 3B), consistent with previous studies indicating little to no actin filaments in the fusome (Warn *et al.*, 1985; Lin *et al.*, 1994). The pres-

ence of detectable actin filaments in spectrosomes but not fusomes suggests that changes in actin filament localization or accessibility normally occur during the spectrosome-to-fusome transition.

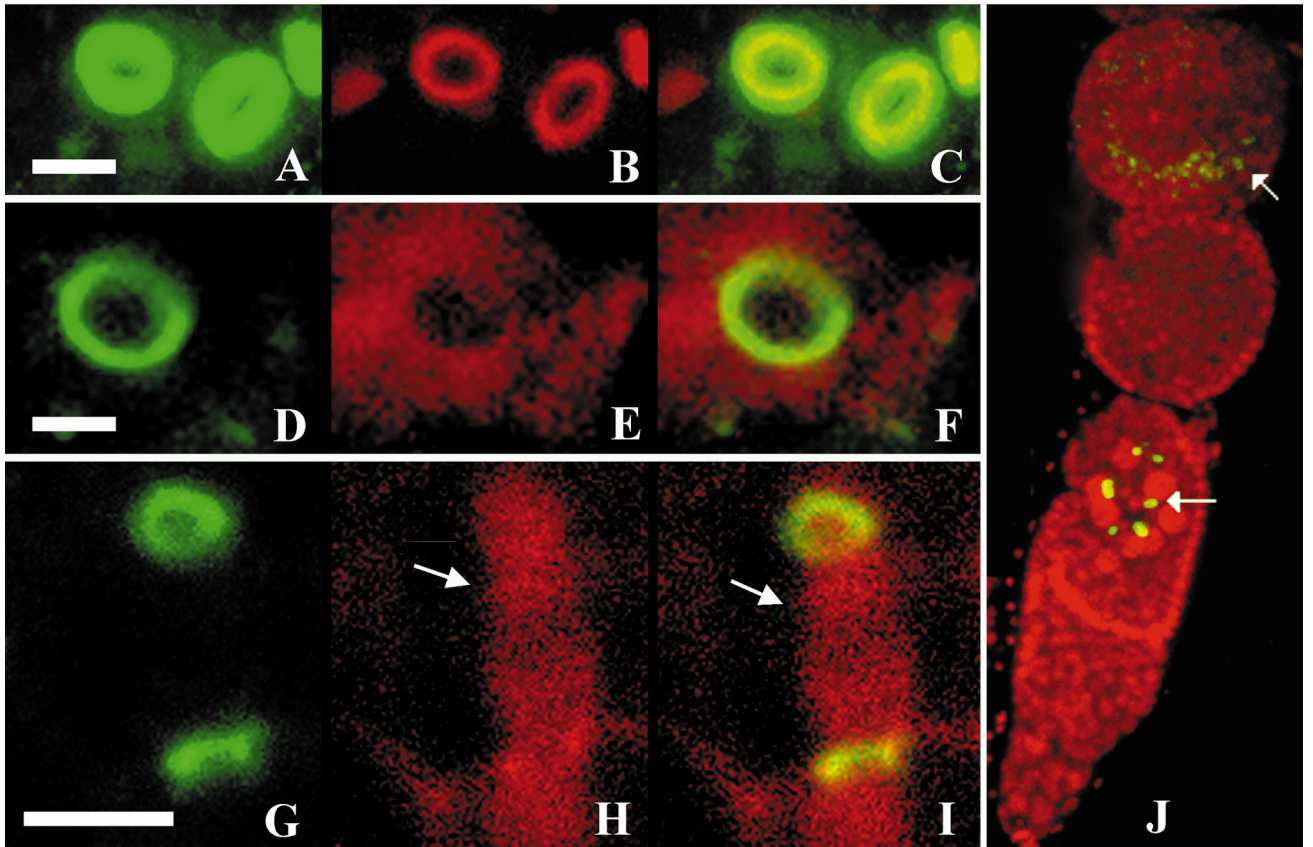
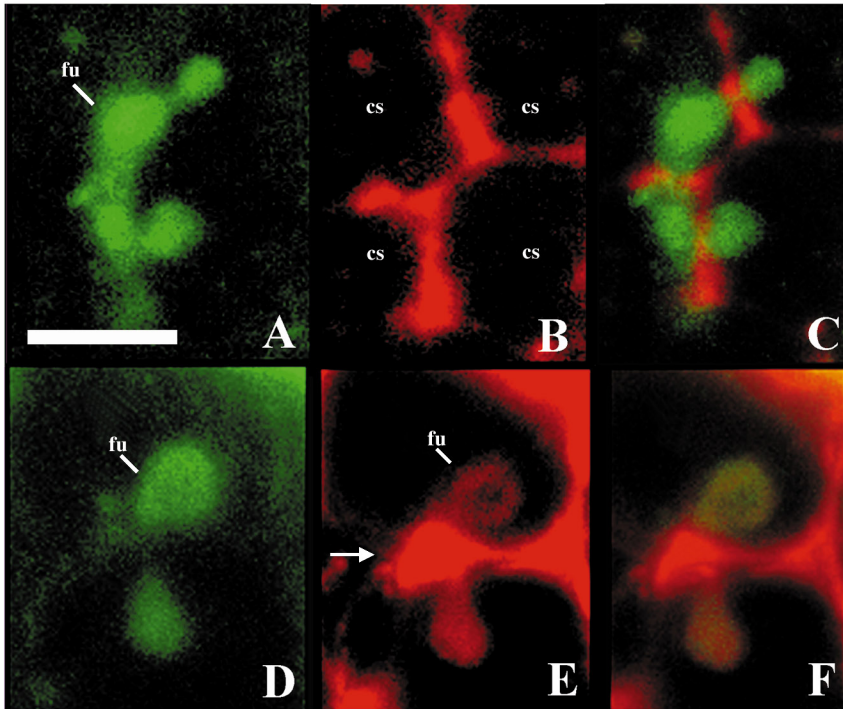
As with wild type, *otu*<sup>PΔ1</sup> mutant fusomes contain spectrin (Fig. 3D), and the mutant cystocytes still have high levels of cortical actin filaments (Fig. 3E). However, in contrast to wild type, substantial levels of actin filaments were detected in all mutant fusomes examined (>25) (Figs. 3E and 3F). These data indicate that *otu* is required for normal fusome structure, in particular actin filament organization or levels during the conversion of a spectrosome to a fusome.

### Hypomorphic Tumorous Alleles Block Inner Rim Formation

To further examine differences between the hypomorphic and null tumor phenotypes, we examined the distribution of actin in the ring canals of tumorous cells mutant for the hypomorphic *otu*<sup>13</sup> allele. In Fig. 4, *otu*<sup>13</sup> ring canals are shown double-labeled with anti-phosphotyrosine antibodies, a marker of ring canals during all oogenic stages, and phalloidin. A range of ring canal phenotypes were observed consistent with the variation seen by electron microscopy (Fig. 2). In a subset of tumorous cystocytes, a phosphotyrosine ring colocalized with an actin ring (Figs. 4A–4C). This is identical to what is observed in region II wild-type ring canals and is indicative of an inner rim containing actin filaments and phosphotyrosine, associated with an outer ring containing phosphotyrosine (Robinson *et al.*, 1994). Another class of tumorous cells were found that failed to form an actin inner rim (Figs. 4D–4F). Instead, actin was present in a diffuse

**FIG. 3.** Double-labeling of fusomes to identify actin and spectrin. Cells were simultaneously labeled with Texas red-phalloidin and anti-spectrin, the latter tagged with FITC-labeled secondary antibodies. Images are from confocal microscopy. (A) FITC channel showing spectrin labeling in a wild-type branched fusome (fu). (B) Same preparation in the Texas red channel showing actin distribution. Note high levels of cortical actin outlining four cystocytes (cs), but no fusome staining. (C) Double-labeling showing the fusome connecting four cystocytes (spectrin in green, actin in red). (D) FITC channel showing spectrin labeling in an *otu*<sup>PΔ1</sup> fusome. (E) Same preparation in the Texas red channel showing actin filaments in fusome and cortical regions. Arrow points to boundary between two cystocytes. (F) Double-labeling showing the fusome connecting two cystocytes. Size bar equals 10 μm for all panels.

**FIG. 4.** Double-labeling of *otu*<sup>13</sup> ring canals to identify phosphotyrosine epitope and actin. Cells were simultaneously labeled with Texas red-phalloidin and anti-phosphotyrosine, the latter tagged with FITC-labeled secondary antibody. Images are magnified ring canals visualized with confocal microscopy. (A) FITC channel showing phosphotyrosine epitope in ring canal rims. (B) Same preparation in the Texas red channel showing actin inner rim. (C) Double-labeling showing overlap (yellow) between the actin (red) and phosphotyrosine (green) rings. (D) FITC channel showing phosphotyrosine epitope in ring canal. (E) Same preparation in the Texas red channel showing cortical actin surrounding the ring canal but being occluded from the central opening. No clearly defined inner rim is apparent. (F) Double-labeling showing regions of overlap. (G) FITC channel showing two phosphotyrosine ring canals from a single cystocyte. This cystocyte has undergone two mitotic divisions. (H) Same preparation in the Texas red channel showing actin filaments in the polyfusome (arrow). (I) Double-labeling showing distribution actin (red) and phosphotyrosine epitope (green). Arrow indicates actin in fusome. (J) Low magnification showing mutant ovariole labeled with propidium iodide (labels nuclei in red) and antibodies for the ring canal specific isoform of the Hts protein (green). Three egg chambers are shown: two at the top are tumorous while the lower one has a nurse-like cell cluster based on nuclei size (lower arrow). Part of germarium is at the bottom. Arrows indicate locations of Hts-positive (green-yellow) ring canal clusters. (A–C) Same magnification; size bar equals 5 μm. (D–F) Same magnification; size bar equals 2 μm. (G–I) Same magnification; size bar equals 5 μm.



halo encircling the phosphotyrosine ring but was excluded from the ring interior (Fig. 4E). In wild-type preparations similar actin halos were observed (data not shown). We interpret this pattern as indicating that even those *otu* mutant ring canals that lack actin inner rims are surrounded by approximately normal levels of cortical actin. A similar range of phenotypes were observed in *otu*<sup>PΔ3</sup> mutants (data not shown).

In addition, many *otu*<sup>13</sup> and *otu*<sup>PΔ3</sup> cystocytes in germaria and tumorous chambers contained fusomes. These probably represent a mixture of germ cells arrested at an early stage (like *otu*<sup>PΔ1</sup> mutants) and those in the process of maturing. In every case examined (>25 germarial cells) the fusomes are similar to *otu*<sup>PΔ1</sup> mutants in that they contain actin filaments. This is even true for the rare polyfusomes that are associated with two or more ring canals (Figs. 4G–4I). In Fig. 4G, two phosphotyrosine rings from a single cystocyte are shown. Extending through the ring canals is a phalloidin-stained fusome (Figs. 4H and 4I). Therefore, despite the additional round of division the polyfusome still has an aberrant structure relative to actin. Our data also confirm an earlier observation about *otu* mutants. Wild-type fusomes extend into adjacent cells at an approximately 135° angle as seen in Fig. 3C, forming a branched structure (Lin and Spradling, 1995). In contrast, the *otu* mutant polyfusomes containing actin filaments are generally linear or unbranched (Fig. 4I; King, 1979).

Not surprisingly, the hypomorphic *otu*<sup>13</sup> and *otu*<sup>PΔ3</sup> mutants also occasionally contained more mature cystocytes, as defined by ring canals associated with the Hts protein (Fig. 4J). Hts normally becomes localized to the ring in region IIa cystocytes (Yue and Spradling, 1992; Lin and Spradling, 1995). Some chambers contained regions of tumorous cells that expressed the Hts protein (Fig. 4J, top arrow), while others had occasional nurse cell clusters with larger, more mature rings (Fig. 4J, lower arrow). In general however, the great majority of cells were tumorous and did not have Hts associated with their ring canals. Hts-associated ring canals were also sporadically seen in *otu*<sup>PΔ1</sup> mutant cells, although at much lower frequencies than observed with the hypomorphic alleles. These occurred as small clusters near the posterior end of the germaria or in the most posterior egg chamber present in the ovariole. We believe these represent older germ cells that have partially escaped the *otu* mutant arrest.

### **Differentiated *otu* Alleles Block Oogenesis before the Dumping Stage**

During stages 10–12 of oogenesis, nonselective transport occurs in which the contents of the nurse cell cytoplasm are transferred to the oocyte. This “dumping” is an actin/myosin-dependent process that initiates during stage 10a (Theurkauf *et al.*, 1992; Cooley and Theurkauf, 1994). The phenotype of the *otu*<sup>7</sup> allele, which arrests oogenesis at about stage 10, led to the suggestion that *otu* function is required for the dumping process (Storto and King, 1988).

To confirm the block in cytoplasmic transport, we utilized the *exu-GFP* construct in which the cnidarian green fluorescent sequence is fused to the *exuperentia* protein (Wang and Hazelrigg, 1994). The Exu-GFP fusion protein is expressed in the nurse cell cytoplasm prior to stage 10 and then gets transported into the oocyte during dumping. In *otu*<sup>7</sup> mutant egg chambers, Exu-GFP mostly remains in the nurse cells (Fig. 5A). In many cases the nurse cell nuclei are misplaced relative to wild type, with some appearing to block ring canal openings (Fig. 5A). This phenotype is similar to that found for several other dumpless mutations that affect germline cytoskeletal elements (Cooley *et al.*, 1992; Mahajan-Miklos and Cooley, 1994). We found that cytoplasmic dumping also fails to occur in *otu*<sup>14</sup>/*otu*<sup>PΔ1</sup>, *otu*<sup>5</sup>/*otu*<sup>5</sup>, and *otu*<sup>PΔ5</sup>/*otu*<sup>PΔ5</sup> mutant chambers (data not shown).

### **Differentiated *otu* Alleles Disrupt Actin Organization in Stage 10 Egg Chambers**

Cytoplasmic dumping during stage 10 is believed to require subcortical actin for nurse cell contraction and a complex array of cytoplasmic actin filaments that anchor the nurse cell nucleus to the plasma membrane (reviewed in Mahajan-Miklos and Cooley, 1994). The latter are believed to prevent the nucleus from blocking the ring canals as the cytoplasm flows toward the oocyte. This actin array can be visualized by phalloidin staining which shows an elaborate set of filaments in stage 10 nurse cells (Fig. 5B) that initially forms on the plasma membrane and rapidly extends to the nucleus (Riparbelli and Callaini, 1995).

It was previously shown that nurse cells mutant for *otu*<sup>7</sup> failed to form this cytoplasmic actin array, although other alleles tested showed a normal phenotype (Storto and King, 1988). To determine whether this actin phenotype was an anomaly specific to the *otu*<sup>7</sup> allele or a more general property of *otu*, we examined ovaries mutant for the hypomorphic *otu*<sup>PΔ5</sup>, *otu*<sup>5</sup>, and *otu*<sup>14</sup> mutations. In each case, there were major disruptions in the cytoplasmic actin cytoskeleton while cortical actin appeared unaffected (data are shown for *otu*<sup>PΔ5</sup>; Fig. 5C). However, in addition to the loss of actin fibers connecting the nucleus to the plasma membrane, we typically observed actin filaments clustering around the nucleus and partially extending to the plasma membrane (Fig. 5C). It therefore appears as if *otu* mutations cause actin polymerization to initiate from the nucleus.

In contrast to actin, there is no indication that myosin distribution is affected by *otu* mutations. Fluorescent antibody labeling reveals a cortical distribution of myosin II at levels indistinguishable from wild type (data not shown).

## **DISCUSSION**

### ***otu* Is Required in at Least Two Germarial Stages**

We compared the phenotypes of three *otu* alleles that have different effects on the two *otu* isoforms but still give

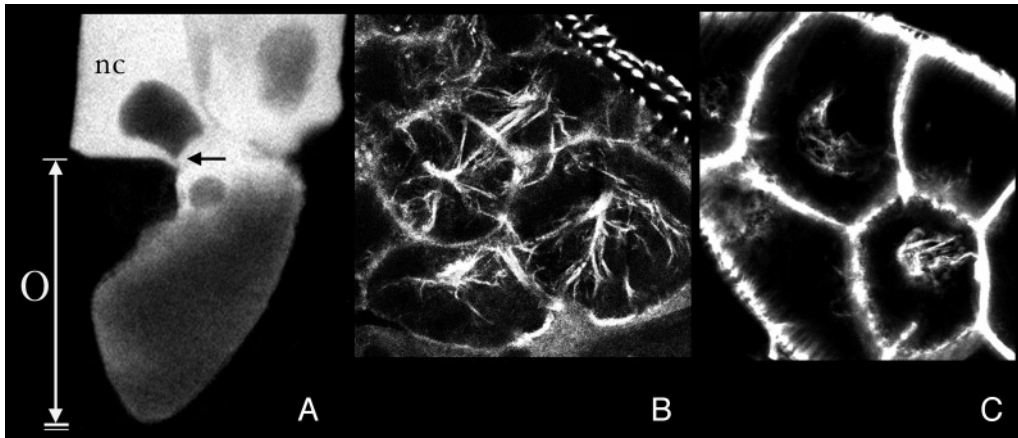


**FIG. 5.** The *otu* dumple phenotype. (A) Confocal image of *otu*<sup>7</sup> stage 10 chamber expressing *exu-GFP* construct in nurse cells (nc). Exu-GFP is present in the cytoplasm but not in the nurse cell nucleus. The arrow points to the nurse cell nucleus being forced into the oocyte (O) ring canal. The oocyte nucleus is visible below the arrow. (B) Confocal image of phalloidin-labeled actin filaments connecting the plasma membrane and nucleus in wild-type stage 10 nurse cells. Both the cytoplasmic array and cortical actin are labeled. (C) Confocal image of phalloidin-labeled actin filaments in *otu*<sup>PΔ5</sup> stage 10 nurse cells. Note the actin filaments clustered on the nuclear membrane but not on the plasma membrane. High levels of cortical actin are present. (B, C) Same magnification.

rise to morphologically similar tumorous egg chambers. These studies demonstrate that (1) *otu* activity is required during at least two germarial stages (if not continuously) and (2) *otu* mutations have differential effects on the number of cystocyte divisions and on cystocyte differentiation.

The *otu*<sup>PΔ1</sup> mutation completely eliminates *otu* activity, producing either agametic ovarioles or tumorous egg chambers. The majority of mutant germ cells are viable and are morphologically similar to either cystoblasts or first-division cystocytes. The lack of cystocytes with multiple ring canals correlates with the immature morphology of the mutant ring canals and the presence of fusomes, both characteristic of cystocyte stages prior to the completion of the cystocyte divisions. Apparently once the mutant cystoblast undergoes the first cystocyte division, mitotic activity typically ceases. Therefore, the overproliferating cells that make up the tumorous chambers and agametic ovarioles are most likely either oogonial stem cells or cystoblasts. This is supported by the observation that many of the tumorous cells that lack ring canals have spectrosomes, a characteristic of oögonia prior to the first cystocyte division (Lin and Spradling, 1995).

A different type of tumorous cell is found in mutants for the hypomorphic *otu*<sup>13</sup> and *otu*<sup>PΔ3</sup> alleles. As with *otu*<sup>PΔ1</sup>, the majority of the *otu*<sup>13</sup> and *otu*<sup>PΔ3</sup> tumorous cells have either zero or one ring canal, although a higher frequency of four- to eight-cell clusters and even a few 16-cell cysts are observed. In comparison to tumorous cells with single ring canals, both *otu*<sup>13</sup> and *otu*<sup>PΔ3</sup> mutants appeared to have reached a more mature developmental stage than *otu*<sup>PΔ1</sup>, with morphologies characteristic of wild-type cystocytes found in region II. Development to this stage would be consistent with the higher frequency of egg chamber formation

in these mutants compared to *otu*<sup>PΔ1</sup>, since it is in region II that interactions with the follicle cell layer normally occur. Furthermore, this increased differentiation is consistent with our previous findings that *otu*<sup>PΔ3</sup> and *otu*<sup>13</sup>, but not *otu*<sup>PΔ1</sup>, can be partially suppressed by overexpression alleles of *Sxl* (Bae *et al.*, 1994). In these cases, the typically tumorous *otu*<sup>13</sup> or *otu*<sup>PΔ3</sup> germ cells mature to late oögonic stages and even produce some functional eggs (Pauli *et al.*, 1993; Bae *et al.*, 1994). We suggest that *otu*<sup>PΔ1</sup> mutants are arrested prior to region II and are consequently not receptive to increased or ectopic *Sxl* expression. In contrast, suppression can occur with those hypomorphic alleles (like *otu*<sup>13</sup> and *otu*<sup>PΔ3</sup>) that allow germ cells to differentiate beyond the region I stage. This correlates with the nuclear localization of the germline *Sxl* protein that first occurs in region II germ cells (Bopp *et al.*, 1993), perhaps becoming biologically active at this stage.

These results illustrate the requirement of *otu* for both cystocyte division and differentiation. In the absence of *otu* activity, only a single cystocyte division typically occurs, rather than the four required to form a 16-cell cyst. The morphology of the cystocytes relative to the fusome and ring canal is consistent with an arrest at this time. However, we found that hypomorphic tumorous alleles can provide sufficient *otu* activity to allow further cystocyte development to a stage characteristic of a 16-cell cystocyte, but without stimulating additional divisions. This indicates that the cystocyte differentiation and proliferation processes can be at least partially uncoupled by *otu* mutations.

#### ***otu* Is Needed for Normal Actin Distribution in Early and Late Oögenesis**

The *otu* gene is required during at least three oögonic stages, the two germarial stages described above and during

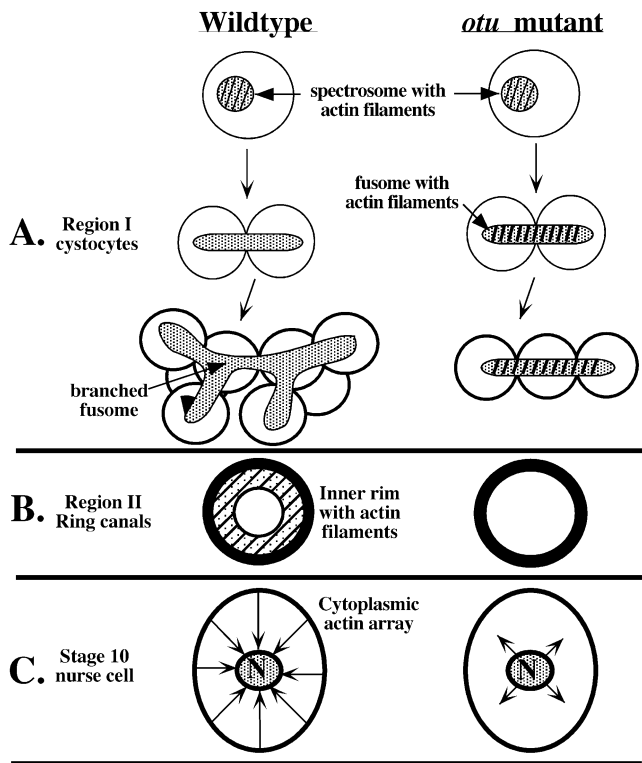


**FIG. 6.** Summary of alterations in actin organization caused by *otu* mutations. (A) Actin filaments (diagonal lines) present in the spectrosome are normally not detected in the fusomes of region I cystocytes. Wild-type polyfusomes are always branched. In *otu* mutants, actin filaments remain in the fusome and, in the rare instances when >2 cystocytes are interconnected, the polyfusomes are unbranched. (B) Wild-type region II cystocytes form ring canals that have an outer rim (black circle) and an inner rim (shaded circle). The inner rim contains actin filaments (diagonal lines; Warn *et al.*, 1985). The ring canals of *otu* mutant tumorous germ cells often fail to form an inner rim. (C) In stage 10 nurse cells, actin bundles (arrows) grow from the plasma membrane to the nuclear membrane to anchor the nucleus (N). In *otu* mutants, actin filaments appear in opposite orientation, forming on the nuclear membrane but failing to extend to the plasma membrane.

nurse cell dumping in stage 10, that result in the three morphologically distinct phenotypic classes described by King and Riley (1982). We found that in each of these stages the distribution of actin filaments is aberrant, although in each case different cytological regions and structures are affected (Fig. 6).

The earliest mutant phenotype occurs about the time that the spectrosome gives rise to the fusome during the first cystocyte division. Normally during this process, actin filaments present in the spectrosome (Fig. 1C) are reduced or modified such that they are no longer detected in the fusome (Lin *et al.*, 1994). In contrast, *otu* mutants cause actin filaments to be present in both the spectrosome and fusome. This could occur if *otu* is required for the normal transition

of the spectrosome to a fusome, perhaps by removing or depolymerizing actin filaments or by modifying the fusome in such a way that actin filaments become inaccessible to phalloidin.

This aberration is particularly interesting because the fusome is associated with two early oogenic processes that are affected by *otu* mutations. First, the fusome may act as a positive regulator of cystocyte division (Lin *et al.*, 1994; Lin and Spradling, 1995). This correlates with the observation that *otu* is required for cystocytes to undergo the four rounds of mitotic divisions needed to make a 16-cell cyst. Second, the fusome appears to be required to orient the mitotic spindle during cystocyte divisions (Lin and Spradling, 1995). Normally, the mitotic spindles are at an angle of approximately 135° from the plane of the fusomes, resulting in branched fusomes with angled arms (Lin and Spradling, 1995). In *otu* mutants, tumorous germ cells will infrequently undergo a second mitotic division to produce a fusome connecting three or more cells (Fig. 4I). In these cases the fusome is often linear and unbranched (Fig. 6A; King, 1979), a phenotype indicative of a mitotic spindle aligned along the same plane as the fusome.

A second aberration in actin distribution is seen in ovaries mutant for the hypomorphic *otu*<sup>13</sup> and *otu*<sup>PΔ3</sup> alleles. Many of the tumorous cells have ring canals that lack fusomes, a phenotype associated with wild-type cystocytes midway in germarial region II. Normally, the loss of the fusome is coincident with the deposition of actin filaments and Hts in the ring canal to form the inner rim (Warn *et al.*, 1985; Robinson *et al.*, 1994; Tilney *et al.*, 1996). However, *otu*<sup>13</sup> and *otu*<sup>PΔ3</sup> ring canals lacking fusomes frequently do not have a clearly defined, actin-associated inner rim (Fig. 2D, Figs. 4D–4F, and Fig. 6B). This actin defect may explain the miniring canals frequently found in *otu*<sup>13</sup> and *otu*<sup>PΔ3</sup> mutants (Fig. 2F). It has been speculated that the expansion of the ring canal during oogenesis occurs by the polymerization of actin from new sites at the membrane, producing bundles of newly formed filaments that slide past existing bundles to increase ring diameter (Tilney *et al.*, 1996). Therefore, mislocalization or disruption of actin filament formation due to *otu* mutations could prevent ring canal expansion once the fusome has regressed.

Perhaps the most dramatic disruption of actin filament formation by *otu* mutations occurs in weak hypomorphic allele combinations that block oogenesis at stage 10, when the nurse cell cytoplasmic contents are nonspecifically “dumped” into the oocyte. Dumping fails to occur in these mutants and the nurse cells fail to form the cytoplasmic actin filament array that anchors the nurse cell nuclei (Storto and King, 1988). In contrast, the levels of subcortical actin appear normal, consistent with *otu* mutations causing specific aberrations in the distribution and organization of actin filaments rather than more general effects on actin levels or polymerization.

We also observed in *otu*<sup>PΔ5</sup>, *otu*<sup>5</sup>, *otu*<sup>7</sup>, and *otu*<sup>14</sup> mutant chambers that actin would frequently aggregate around the nurse cell nucleus without extending to the plasma mem-

brane. This suggests that actin polymerization initiates at the nucleus. In contrast, in wild-type chambers at this stage actin bundles radiate from the cortical cytoplasm and terminate at the nuclear envelop (Riparbelli and Callaini, 1995). A similar actin aggregation pattern is seen in ovaries mutant for the *stand still* gene which has mutant phenotypes similar to that found in *otu* (Mulligan *et al.*, 1996).

A dumpless phenotype similar to that seen with *otu* mutants is produced by other mutations that disrupt the actin cytoskeleton. These include mutations in genes encoding known actin-binding proteins, such as *chickadee* (profilin; Cooley *et al.*, 1992), *quail* (villin; Mahajan-Miklos and Cooley, 1994), and *singed* (fascin; Cant *et al.*, 1994), as well as in the *Drosophila*  $\beta$ -catenin *armadillo* gene (Peifer *et al.*, 1993). In each case, the actin microfilament array fails to form during oogenic stage 10b. These data are consistent with the *otu* dumpless phenotype being a direct consequence of abnormal actin organization.

However, the *otu* gene differs from these actin-associated dumpless genes in two respects. First, mutations in these dumpless genes do not give rise to tumorous egg chambers. Similarly, mutations in genes that disrupt the formation of the fusome and ring canals, such as *hts* and *kelch*, also fail to produce phenotypes similar to *otu* null mutants and do not disrupt the stage 10 cytoskeletal array (Yue and Spradling, 1992; Xue and Cooley, 1993). Therefore, *otu* has a broader effect on actin distribution in oogenesis than any of the previously described dumpless and ring canal genes. Second, the detection of actin filaments in *otu*<sup>P $\Delta$ 1</sup> fusomes indicates that *otu* mutations do not prevent actin polymerization, but rather seem to alter the location where actin filaments either form or accumulate. This could explain how *otu* mutations can cause ectopic accumulation of filaments in the cystocyte fusome and along stage 10 nurse cell nuclear membranes, but prevent actin filament association with the developing ring canal and the plasma membranes of stage 10 nurse cells.

In summary, we have described the first common molecular defect linking the *otu* agametic, tumorous, and differentiated phenotypes. In each oogenic stage affected by *otu* mutations, it appears that the association of actin with specific structures is aberrant. Actin microfilaments are inappropriately placed in the fusome, fail to associate with ring canals, or fail to connect the nucleus to the plasma membrane (Fig. 6). This effect of *otu* mutations on actin is sex-specific and dosage-dependent, with greater *otu* activity needed as the eggs mature.

## ACKNOWLEDGMENTS

We are grateful for the comments of Joe Frankel and Wayne Johnson concerning the manuscript. In addition, we extend our thanks to Dan Branton, Doug Robinson, and Lynn Cooley for providing antibodies. Thanks to Jim Skinner and Dean Abel for advice and technical assistance with the transmission EM work in this article.

This work was supported by grants from the National Institutes of Health, the Carver Foundation, and the CIFRE fund.

## REFERENCES

- Bae, E., Cook, K. R., Geyer, P. K., and Nagoshi, R. N. (1994). Molecular characterization of ovarian tumors in *Drosophila*. *Mech. Dev.* **47**, 151–164.
- Bishop, D. L., and King, R. C. (1984). An ultrastructural study of ovarian development in the *otu*<sup>7</sup> mutant of *Drosophila melanogaster*. *J. Cell Sci.* **67**, 87–119.
- Bopp, D., Horabin, J. I., Lersch, R. A., Cline, T. W., and Schedl, P. (1993). Expression of the *Sex-lethal* gene is controlled at multiple levels during *Drosophila* oogenesis. *Development* **118**, 797–812.
- Cant, K., Knowles, B., Mooseker, M., and Cooley, L. (1994). *Drosophila* *singed*, a fascin homolog, is required for actin bundle formation during oogenesis and bristle extension. *J. Cell Biol.* **125**, 369–380.
- Cooley, L., and Theurkauf, W. E. (1994). Cytoskeletal functions during *Drosophila* oogenesis. *Science* **266**, 590–596.
- Cooley, L., Verheyen, E., and Ayers, K. (1992). *chickadee* encodes a profilin required for intercellular cytoplasm transport during *Drosophila* oogenesis. *Cell* **69**, 173–184.
- Edwards, K. A., and Kiehart, D. P. (1996). *Drosophila* nonmuscle myosin II has multiple essential roles in imaginal disc and egg chamber morphogenesis. *Development* **122**, 1499–1511.
- Geyer, P. K., Patton, J. S., Rodesch, C., and Nagoshi, R. N. (1993). Genetic and molecular characterization of *P* element-induced mutations reveals that the *Drosophila* *ovarian tumor* gene has maternal activity and a variable null phenotype. *Genetics* **133**, 265–278.
- King, R. C. (1970). "Ovarian Development in *Drosophila melanogaster*." Academic Press, New York.
- King, R. C. (1979). Aberrant fusomes in the ovarian cystocytes of the *fs(1)231* mutant of *Drosophila melanogaster* Meigen (Diptera: Drosophilidae). *Int. J. Insect Morphol. Embryol.* **8**, 297–309.
- King, R. C., Mohler, J. D., Riley, S. F., Storto, P. D., and Nicolazzo, P. S. (1986). Complementation between alleles at the *ovarian tumor (otu)* locus of *Drosophila melanogaster*. *Dev. Genet.* **7**, 1–20.
- King, R. C., and Riley, S. F. (1982). Ovarian pathologies generated by various alleles of the *otu* locus in *Drosophila melanogaster*. *Dev. Genet.* **3**, 69–89.
- King, R. C., and Storto, P. D. (1988). The role of the *otu* gene in *Drosophila* oogenesis. *Bioessays* **8**, 18–24.
- Koch, E. A., and King, R. C. (1969). Further studies on the ring canal system of the ovarian cystocytes of *Drosophila melanogaster*. *Z. Zellforsch.* **102**, 129–152.
- Lin, H., and Spradling, A. C. (1995). Fusome asymmetry and oocyte determination in *Drosophila*. *Dev. Genet.* **16**, 6–12.
- Lin, H., Yue, L., and Spradling, A. C. (1994). The *Drosophila* fusome, a germline-specific organelle, contains membrane skeletal proteins and functions in cyst formation. *Development* **120**, 947–956.
- Lindsley, D. L., and Zimm, G. (1992). "The Genome of *Drosophila melanogaster*." Academic Press, San Diego.
- Mahajan-Miklos, S., and Cooley, L. (1994). Intercellular cytoplasm transport during *Drosophila* oogenesis. *Dev. Biol.* **165**, 336–351.
- Mahajan-Miklos, S., and Cooley, L. (1994). The villin-like protein encoded by the *Drosophila* *quail* gene is required for actin bundle assembly during oogenesis. *Cell* **78**, 291–301.

- Mahowald, A. P. (1971). The formation of ring canals by cell furrows in *Drosophila*. *Z. Zellforsch.* **118**, 162–167.
- Mahowald, A. P., and Kambyssellis, M. P. (1980). In "Genetics and Biology of *Drosophila*" (M. Ashburner and T. R. F. Wright, Eds.), pp. 141–224. Academic Press, New York.
- McKearin, D., and Ohlstein, B. (1995). A role for the *Drosophila* Bag-of-marbles protein in the differentiation of cystoblasts from germline stem cells. *Development* **121**, 2937–2947.
- McKearin, D. M., and Spradling, A. C. (1990). *bag-of-marbles*: A *Drosophila* gene required to initiate both male and female gametogenesis. *Genes Dev.* **4**, 2242–2251.
- Meyer, G. F., Hess, O., and Beermann, W. (1961). Phasenspezifische funktionsstrukturen in spermatocytenkernen von *Drosophila melanogaster* und ihre abhangigkeit vom Y-chromosom. *Chromosoma* **12**, 676–716.
- Mulligan, P. K., Campos, A. R., and Jacobs, J. R. (1996). Mutations in the gene stand still disrupt germ cell differentiation in *Drosophila* ovaries. *Dev. Genet.* **18**, 316–326.
- Oliver, B., Kim, Y.-J., and Baker, B. S. (1993). Sex-lethal, master and slave: A hierarchy of germ-line sex determination in *Drosophila*. *Development* **119**, 897–908.
- Pauli, D., Oliver, B., and Mahowald, A. P. (1993). The role of the *ovarian tumor* locus in *Drosophila melanogaster* germ line sex determination. *Development* **119**, 123–134.
- Peifer, M., Orsulic, S., Sweeten, D., and Wieschaus, E. (1993). A role for the *Drosophila* segment polarity gene *armadillo* in cell adhesion and cytoskeletal integrity during oogenesis. *Development* **118**, 1191–1207.
- Reynolds, E. S. (1963). The use of lead citrate at high pH as an electron opaque stain in electron microscopy. *J. Cell Biol.* **17**, 208–212.
- Riparbelli, M. G., and Callaini, G. (1995). Cytoskeleton of the *Drosophila* egg chamber: New observations on microfilament distribution during oocyte growth. *Cell Motil. Cytoskel.* **31**, 298–306.
- Robinson, D., Cant, K., and Cooley, L. (1994). Morphogenesis of *Drosophila* ring canals. *Development* **120**, 2015.
- Rodesch, C., Geyer, P. K., Patton, J. S., and Nagoshi, R. N. (1995). Developmental analysis of the *ovarian tumor* and *ovo* genes during *Drosophila* oogenesis. *Genetics* **141**, 191–202.
- Sass, G. L., Comer, A. R., and Searles, L. L. (1995). The ovarian tumor protein isoforms of *Drosophila melanogaster* exhibit differences in function, expression, and localization. *Dev. Biol.* **167**, 201–212.
- Sass, G. L., Mohler, J. D., Walsh, R. C., Kalfayan, L. J., and Searles, L. L. (1993). Structure and expression of hybrid dysgenesis-induced alleles of the *ovarian tumor* (*otu*) gene in *Drosophila melanogaster*. *Genetics* **133**, 253–263.
- Spradling, A. C. (1993). Germline cysts: Communes that work. *Cell* **72**, 649–651.
- Steinhauer, W., and Kalfayan, L. J. (1992). A specific *ovarian tumor* protein isoform is required for efficient differentiation of germ cells in *Drosophila* oogenesis. *Genes Dev.* **6**, 233–243.
- Steinhauer, W. R., Walsh, R. C., and Kalfayan, L. J. (1989). Sequence and structure of the *Drosophila melanogaster ovarian tumor* gene and generation of an antibody specific for the ovarian tumor protein. *Mol. Cell. Biol.* **9**, 5726–5732.
- Steinmann-Zwicky, M. (1992). Sex determination of *Drosophila* germ cells. *Semin. Dev. Biol.* **3**, 341–347.
- Storto, P. D., and King, R. C. (1988). A multiplicity of functions for the *otu* gene products during *Drosophila* oogenesis. *Dev. Genet.* **9**, 91–120.
- Theurkauf, W. E., Smiley, S., L. W. M., and Alberts, B. M. (1992). Reorganization of the cytoskeleton during *Drosophila* oogenesis: Implications for axis specification and intercellular transport. *Development* **115**, 923–936.
- Tilney, L. G., Tilney, M. S., and Guild, G. M. (1996). Formation of actin filament bundles in the ring canals of developing *Drosophila* follicles. *J. Cell Biol.* **133**, 61–74.
- Tirronen, M., Lahti, V.-P., Heino, T. I., and Roos, C. (1995). Two *otu* transcripts are selectively localised in *Drosophila* oogenesis by a mechanism that requires a function of the *otu* protein. *Mech. Dev.* **52**, 65–75.
- Wang, S., and Hazelrigg, T. (1994). Implications for *bcd* mRNA localization from spatial distribution of *exu* protein in *Drosophila* oogenesis. *Nature* **369**, 400–403.
- Warn, R. M., Gutzeit, H. O., Smith, L., and Warn, A. (1985). F-actin rings are associated with the ring canals of the *Drosophila* egg chamber. *Exp. Cell Res.* **157**, 355–363.
- Wei, G., Oliver, B., Pauli, D., and Mahowald, A. P. (1994). Evidence for sex transformation of germline cells in ovarian tumor mutants of *Drosophila*. *Dev. Biol.* **161**, 318–320.
- Xue, F., and Cooley, L. (1993). *kelch* encodes a component of intercellular bridges in *Drosophila* egg chambers. *Cell* **72**, 681–693.
- Yue, L., and Spradling, A. C. (1992). *hu-li tai shao*, a gene required for ring canal formation during *Drosophila* oogenesis, encodes a homolog of adducin. *Genes Dev.* **6**, 2443–2454.

Received for publication June 2, 1997

Accepted July 16, 1997